Supporting Information:

Surface Dipole Control of Liquid Crystal Alignment

Jeffrey J. Schwartz,[†,‡] Alexandra M. Mendoza,[†,§] Natcha Wattanatorn,[†,§] Yuxi Zhao,[†,§] Vinh T. Nguyen,[§] Alexander M. Spokoyny,[*,§,⊥] Chad A. Mirkin,[*,⊥] Tomáš Baše,[*,∥] and Paul S. Weiss[*,†,§,¶]

[†]California NanoSystems Institute, University of California, Los Angeles, Los Angeles, California 90095, United States

[‡]Department of Physics & Astronomy, University of California, Los Angeles, Los Angeles, California 90095, United States

[§]Department of Chemistry & Biochemistry, University of California, Los Angeles, Los Angeles, California 90095, United States

[⊥]Department of Chemistry and the International Institute for Nanotechnology, Northwestern University, Evanston, Illinois 60208, United States

[∥]Institute of Inorganic Chemistry, Academy of Sciences of the Czech Republic, v.v.i. 250 68 Husinec-Řež, č.p. 1001, Czech Republic

[¶]Department of Materials Science & Engineering, University of California, Los Angeles, Los Angeles, California 90095, United States

SUPPORTING INFORMATION CONTENTS:

Physical Properties of Liquid Crystals.

Relevant physical properties of the liquid crystals (LCs) used in this work, 4-cyano-4′-pentylbiphenyl (**5CB**) and *N*-(4-methoxybenzylidene)-4-butylaniline (**MBBA**), are summarized in Table S1.

Table S1. Physical properties of 5CB[a] and MBBA[b] liquid crystals.

Property[c]	Liquid Crystals	
	5CB[d]	MBBA[e]
Δn[f]	0.1873	0.184
$\Delta\varepsilon$[g]	+11.5	-0.5
K_{22} (pN)[h]	4.22	4.0
T_{NI} (°C)[i]	35	47
μ (D)[j]	5.1	2.2

[a]4-cyano-4′-pentylbiphenyl (**5CB**). [b]*N*-(4-methoxybenzylidene)-4-butylaniline (**MBBA**). [c]The values of these properties depend on the specific measurement conditions (e.g., temperature, optical wavelength, and chemical purity). Here, we report values applicable to this work. [d]See Refs. S1–4. [e]See Refs. S5–7. [f]Birefringence (Δn), calculated as the difference in the indices of refraction of light polarized along the mesogen's extraordinary and ordinary axes. [g]Dielectric anisotropy ($\Delta\varepsilon$), calculated as the difference in the mesogen's dielectric constant parallel and perpendicular to the director. [h]Mesogen twist elastic constant (K_{22}). [i]Transition temperature (T_{NI}) between the nematic and isotropic phases. [j]Permanent molecular dipole moment (μ) of the mesogen. The dipole moment of **5CB** lies along its molecular axis, whereas the dipole moment of **MBBA** is directed primarily perpendicular to its long axis.

MBBA Cell Rotation–Transmittance Spectra.

Figure S1 shows the modulation in the intensity of the light transmitted through **MBBA** cells as they were rotated between crossed polarizers (Figure 2B). Alignment layers treated with *m*-9-carboranethiol (**M9**), *m*-1-carboranethiol (**M1**), *o*-9-carboranethiol (**O9**), *o*-1-carboranethiol (**O1**), and *o*-9,12-carboranedithiol (**9O12**) SAMs induced uniaxial planar alignment in **MBBA** cells, as indicated by the four-fold symmetry of their transmittance spectra. Cells constructed without a twist in their nematic directors vary from nearly extinguishing all transmitted light to transmitting ~50%. By contrast, cells that possess a 90° twist in their directors have transmittances varying from ~50% to nearly 100%, due to the rotation of the polarization of the transmitted light as it traverses the cell.

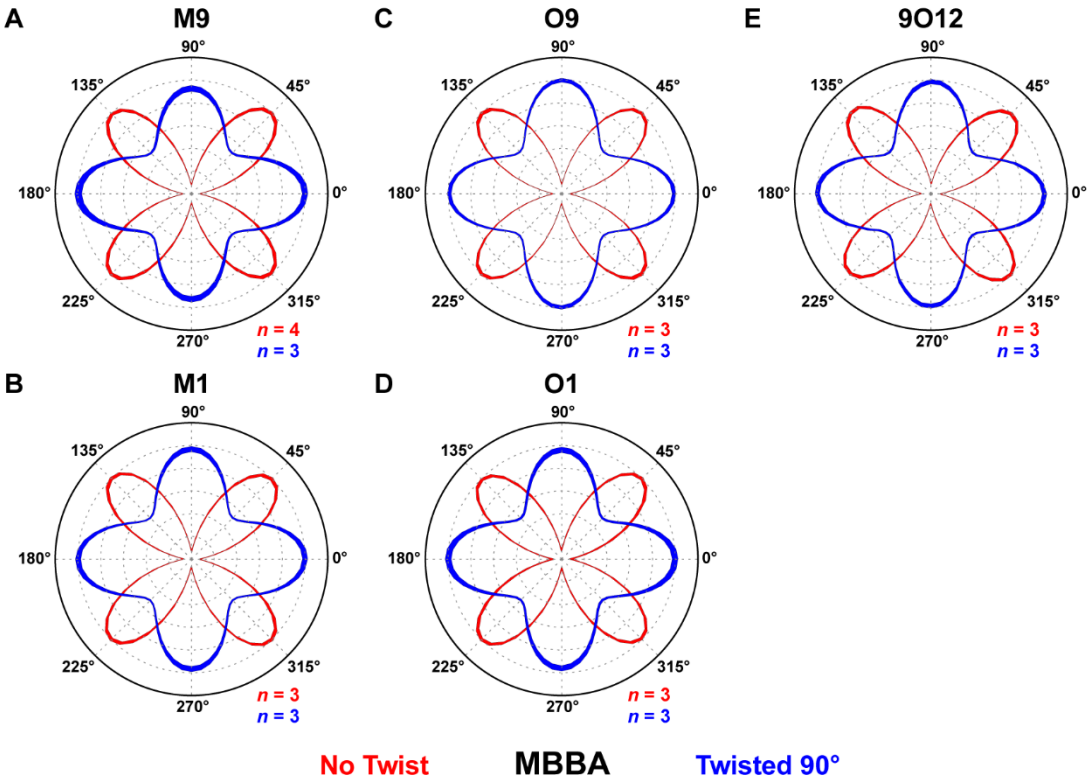

Figure S1. Optical transmittances (indicated by the radial distance from the origin, in arbitrary units) of liquid crystal (LC) cells rotated between crossed polarizers. Alignment layers were prepared with matching self-assembled monolayers of *m*-9-carboranethiol (**M9**), *m*-1-carboranethiol (**M1**), *o*-9-carboranethiol (**O9**), *o*-1-carboranethiol (**O1**), and *o*-9,12-carboranedithiol (**9O12**), as indicated. At these surfaces, uniaxial, planar alignment was manifest in *N*-(4-methoxybenzylidene)-4-butylaniline (**MBBA**) LCs, as evidenced by the variations in optical transmittance possessing four-fold rotational symmetry. Cells were constructed with 0° or 90° angles between their alignment layers' gold deposition axes, producing untwisted (red) or twisted (blue) nematic structures, respectively. Initially, one or both of a cell's gold deposition axes were aligned with the polarizer axis, defined to be at 0°. Rotation angles were measured with respect to this reference orientation, incremented in 5° steps. Reported spectra are averages of analyses performed on n separate LC cells, each consisting of three measured regions, where the radial line widths indicate the data's standard deviation. Spectra are scaled such that their respective transmittance maxima are equal; in actuality, the maximum transmittance of an untwisted nematic cell nearly equals the minimum transmittance of a cell with a 90° twist in its director.

MBBA Cell Voltage–Transmittance Spectra.

Applying a potential difference between the alignment layers generates an electric field that can distort the LC alignment. Mesogens with negative dielectric anisotropies ($\Delta\varepsilon < 0$) adopt an orientation perpendicular to the applied field. In the case of **MBBA**, such fields would induce (or reinforce) planar alignment, parallel to the surface. Any reorientation of the mesogens upon the application of an electric potential ($V_{AC} \leq 7$ V) would alter the transmittances of LC cells viewed between crossed polarizers. As seen in Figure S2, transmittances of cells containing **MBBA** remain constant, indicating prior planar alignment of the mesogens and no subsequent reorientation.

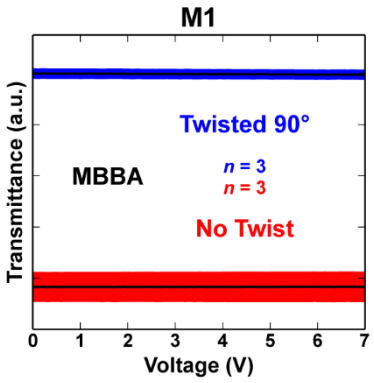

Figure S2. Normalized optical transmittances of electrically modulated liquid crystal (LC) cells viewed between crossed polarizers. Alignment layers were prepared with matching self-assembled monolayers of *m*-1-carboranethiol (**M1**), which induced uniaxial planar alignment in *N*-(4-methoxybenzylidene)-4-butylaniline (**MBBA**) LCs. Cells were constructed with 0° or 90° angles between their alignment layers' gold deposition axes, producing untwisted (red) or twisted (blue) nematic structures, respectively. Cells were positioned between crossed polarizers such that their zero-voltage optical transmittance was maximized (minimized) for twisted (untwisted) nematic structures. Subsequently, a sinusoidally varying (1 kHz) voltage was applied between the alignment layers. Root-mean-square voltages, varied in 0.1 V steps, are indicated along the horizontal axes. Reported spectra are averages (black lines) of analyses performed on $n = 3$ separate LC cells, of each type, where the vertical widths of the surrounding blue outlines indicate the data's standard deviation. No changes in the transmittance spectra were observed with increasing voltage, indicating that the **MBBA** mesogens did not reorient as a result of the applied electric field.

MBBA Anchoring Orientation Cells.

Anchoring orientation wedge cells were used to determine the in-plane orientation of **MBBA** LCs relative to the oblique gold deposition direction ($\overrightarrow{\mathbf{Au}}$): parallel or perpendicular. As shown in Figure S3, the fringes observed in cells made using **M1**, **M9**, and **O1** shift toward the thinner ends of the wedges with increased optical retardation along the gold deposition axis, indicating that the **MBBA** nematic director is aligned parallel to $\overrightarrow{\mathbf{Au}}$. By contrast, cells made with **O9** and **9O12** exhibited planar alignment of **MBBA** perpendicular to $\overrightarrow{\mathbf{Au}}$, as evident from the observed fringe shifts toward the thicker ends of the wedges. As such, the orientations of the **MBBA** director match those of **5CB** on alignment layers treated with **M1**, **O1**, **O9**, and **9O12** SAMs. However, in the case of **M9** SAMs, **5CB** and **MBBA** LCs were observed to align along

opposite directions, planar alignment perpendicular and parallel to $\overrightarrow{\mathbf{Au}}$, respectively. We attribute this discrepancy to relatively weak interactions of the **M9** molecular dipole moment with **MBBA** mesogens, in comparison to those of other carboranethiol isomers, and other factors contributing to LC alignment that are always present in each cell, though presumed consistent.

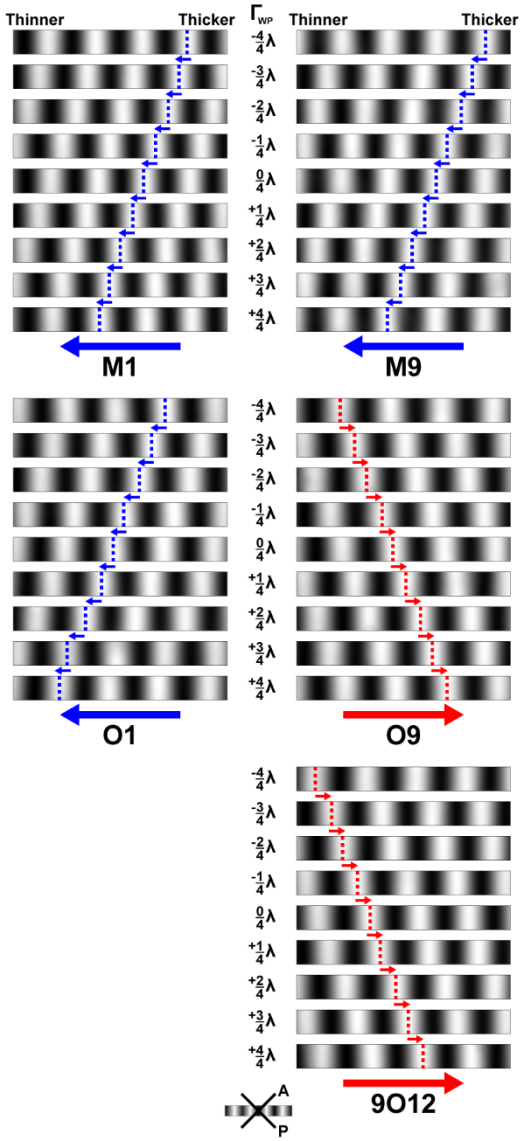

Figure S3. Transmission fringes observed in liquid crystal (LC) wedge cells viewed between crossed polarizers while illuminated with monochromatic light (wavelength $\lambda = 531$ nm). Alignment layers prepared with matching self-assembled monolayers of *m*-1-carboranethiol (**M1**), *m*-9-carboranethiol (**M9**), *o*-1-carboranethiol (**O1**), *o*-9-carboranethiol (**O9**), and *o*-9,12-carboranedithiol (**9O12**), as indicated, induced uniaxial planar alignment of *N*-(4-methoxybenzylidene)-4-butylaniline (**MBBA**) LCs. Wave plates inserted between the polarizers modified the optical retardation of light transmitted through the cells by fixed amounts (Γ_{WP}). Here, positive (negative) values of Γ_{WP} signify that a wave plate's optically slow axis was aligned parallel (perpendicular) to a cell's gold evaporation direction ($\overrightarrow{\mathbf{Au}}$). Arrows and dashed lines track transmittance maxima of constant order within 4.8 mm × 0.5 mm fields of view.

Fringes in cells containing **M1**, **M9**, and **O1** monolayers were observed to shift toward the thinner ends of the wedges with increasing Γ_{WP} (blue), indicating that their nematic directors were oriented parallel to $\overrightarrow{\mathbf{Au}}$. By contrast, fringes shifted toward the thicker ends of wedges containing **O9** and **9O12** monolayers (red), indicating director alignment perpendicular to $\overrightarrow{\mathbf{Au}}$.

5CB Cell Voltage–Transmittance Spectra.

Figure S4 depicts the normalized optical transmittances of untwisted **5CB** cells modulated by an electric field. The scaling applied to these spectra exaggerates the apparent variations in the measured transmittances. Comparing absolute transmittances, the change observed in untwisted **5CB** cells is only about 10% of that seen in **5CB** cells with 90° twists in their directors (Figure 4). The observed transmittance variations in these cells is similar to those expected from untwisted **5CB** cells using other LC alignment techniques (e.g., rubbed polyimide).

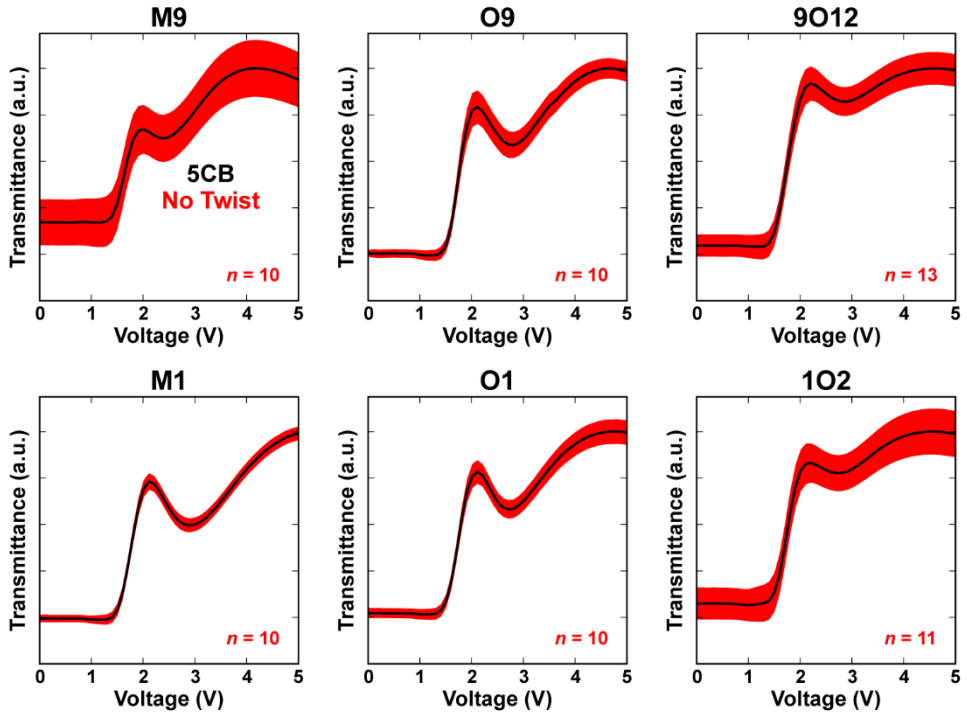

Figure S4. Normalized optical transmittances of electrically modulated liquid crystal (LC) cells viewed between crossed polarizers. Alignment layers were prepared with matching self-assembled monolayers of *m*-9-carboranethiol (**M9**), *m*-1-carboranethiol (**M1**), *o*-9-carboranethiol (**O9**), *o*-1-carboranethiol (**O1**), *o*-9,12-carboranedithiol (**9O12**), and *o*-1,2-carboranedithiol (**1O2**), as indicated. These surfaces induced uniaxial planar alignment in 4-cyano-4′-pentylbiphenyl (**5CB**) LCs. Cells were constructed with parallel gold deposition axes, producing untwisted nematic structures, and were positioned between crossed polarizers such that their zero-voltage optical transmittance was minimized. Subsequently, a sinusoidally varying (1 kHz) voltage was applied between the alignment layers in order to distort the LC director away from the surface. Root-mean-square voltages, varied in 0.1 V steps, are indicated along the horizontal axes. Reported spectra are averages (black lines) of analyses performed on n separate

LC cells, where the vertical widths of the surrounding red outlines indicate the data's standard deviation.

Azimuthal Anchoring Energy.

Azimuthal anchoring energies (W_{az}) of **5CB** aligned by SAMs composed of **M1**, **O9**, **O1**, and **9O12** isomers were measured using the torque balanced method described by Abbott and coworkers.[S4] Here, we summarize the methods used to determine the parameters d, φ, and Ψ in Eq. 2. All measurements were made on anchoring energy wedge cells (Figure 2D) viewed between crossed polarizers. Wedge thicknesses (d) were estimated by comparing the observed (transmitted) color of the cells, illuminated with white light polarized ±45° from their optical axes, to a Michel-Lévy interference color chart,[S8] and then refined using Eq. 1 and the positions of the transmission fringes made visible using monochromatic light ($\lambda = 531$ nm).

We calculated φ and Ψ using the values of δ and γ (Figure S4), which were determined by monitoring the transmission of light through each of the three nematic regions within an anchoring energy cell. The easy alignment axis of the bottom carboranethiol alignment layer ($\boldsymbol{\eta_0}$-bottom) was found by rotating the cell with respect to crossed polarizers while examining an untwisted nematic region. There, transmission minima occur when $\boldsymbol{\eta_0}$-bottom coincides with either of the polarizer or analyzer axes. After aligning $\boldsymbol{\eta_0}$-bottom with the polarizer, the easy axis of the top carboranethiol alignment layer ($\boldsymbol{\eta_0}$-top) was identified by rotating the analyzer with respect the fixed cell until the intensity of light transmitted through the second untwisted nematic region was minimized. In doing so, the analyzer was aligned perpendicular to $\boldsymbol{\eta_0}$-top. The relative angle formed between the polarizer and analyzer axes equaled δ. Finally, the optical transmittance in the central, twisted nematic, region was minimized by, again, rotating the analyzer while keeping the cell orientation fixed. In this configuration, the analyzer was orthogonal to the equilibrium orientation of the director anchored by the top alignment layer ($\boldsymbol{\eta_d}$-top), and the angle formed between the analyzer and polarizer axes equaled γ.

Once δ and γ were determined, the angle (φ) by which the azimuthal orientation of the director departs from the easy alignment axes and the angular twist (Ψ) of the director through the cell's thickness were found using the equations:

$$\varphi = \delta - (\gamma - 90°)$$

$$\Psi = 2(\gamma - 90°) - \delta$$

The anchoring energies reported in Table 1 represent a weighted average of measurements made on multiple cells (at least four of a given isomer) and multiple areas within each cell (up to 10). We computed the uncertainties (σ) of d, φ, and Ψ using the following equations:

$$\sigma_d = \frac{\sigma_\Gamma}{\Delta n}$$

$$\sigma_\varphi = \sqrt{\sigma_\delta^2 + \sigma_\gamma^2}$$

$$\sigma_\Psi = \sqrt{\sigma_\delta^2 + (2\sigma_\gamma)^2}$$

The partial derivatives of W_{az} were found with respect to φ, Ψ, and d, as shown below:

$$\frac{\partial W_{az}}{\partial \Psi} = \frac{2K_{22}}{d\,\sin(2\varphi)}$$

$$\frac{\partial W_{az}}{\partial \varphi} = \frac{-4K_{22}\Psi}{d\,\tan(2\varphi)\,\sin(2\varphi)}$$

$$\frac{\partial W_{az}}{\partial d} = \frac{-2K_{22}\Psi}{d^2\,\sin(2\varphi)}$$

These quantities, evaluated using the parameters of each measurement, were then used to compute the uncertainty in W_{az} ($\sigma_{W_{az}}$):

$$\sigma_{W_{az}} = \sqrt{\left(\frac{\partial W_{az}}{\partial \Psi}\sigma_{\Psi}\right)^2 + \left(\frac{\partial W_{az}}{\partial \varphi}\sigma_{\varphi}\right)^2 + \left(\frac{\partial W_{az}}{\partial d}\sigma_{d}\right)^2}$$

The weighted average of W_{az} and $\sigma_{W_{az}}$ were calculated for i independent measurements using:

$$\text{Weighted Average } W_{az} = \left.\sum_i \frac{W_{az_i}}{\sigma^2_{W_{az_i}}}\right/ \sum_i \frac{1}{\sigma^2_{W_{az_i}}}$$

$$\text{Weighted Average } \sigma_{W_{az}} = \left. 1 \right/ \sqrt{\sum_i \frac{1}{\sigma^2_{W_{az_i}}}}$$

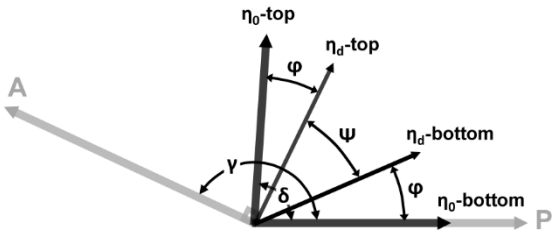

Figure S5. Schematic illustrating the angles used to compute the azimuthal anchoring energy. Orientations of the polarizer and analyzer are denoted by P and A, respectively. Easy alignment axes are indicated for the top (**η_0**-top) and bottom (**η_0**-bottom) alignment layers, while **η_d**-top and **η_d**-bottom indicate the equilibrium director orientations at the top and bottom alignment surfaces, respectively, as a result the opposing torques acting on the twisted nematic. The angle by which the azimuthal orientation of the director deviates from the easy axes is denoted by φ, whereas Ψ is the twist in the LC director between the top and bottom alignment surfaces. Figure adapted with permission from Ref. S4. Copyright 2006 American Chemical Society.

Table S2. Azimuthal anchoring energy (W_{az}) of 4-cyano-4′-pentylbiphenyl (5CB) liquid crystals in cells prepared with *m*-1-carboranethiol (M1) SAMs.

M1		Γ (nm)[a]	δ (°)[b]	γ (°)[c]	W_{az} (μJ·m^{-2})
Sample 1	Spot 1	1590	86.1	1.6	24 ± 3
	Spot 2	2120	86.2	0.8	21 ± 3
Sample 2	Spot 1	800	89.2	1.7	160 ± 30
	Spot 2	1060	89.0	1.2	90 ± 30
	Spot 3	1330	81.8	5.5	11 ± 1
	Spot 4	1590	88.6	1.3	49 ± 13
	Spot 5	1860	88.4	1.4	37 ± 9
	Spot 6	2120	88.5	0.9	41 ± 12
Sample 3	Spot 1	1860	88.0	1.3	35 ± 8
	Spot 2	2120	87.7	2.8	19 ± 3
Sample 4	Spot 1	800	89.1	1.5	110 ± 30
	Spot 2	1060	89.4	1.3	110 ± 40
	Spot 3	1330	89.6	1.0	120 ± 60
	Spot 4	1590	89.8	1.1	110 ± 60
	Spot 5	1860	89.8	0.6	150 ± 140
	Spot 6	2120	89.7	0.9	85 ± 51
	Spot 7	2390	89.9	0.4	180 ± 270
Sample 5	Spot 1	800	86.3	2.0	46 ± 6
	Spot 2	1060	85.0	3.3	24 ± 2
	Spot 3	1330	86.0	2.7	24 ± 3
	Spot 4	1590	85.6	2.9	18 ± 2
	Spot 5	1860	85.5	2.3	16 ± 2
	Spot 6	2120	85.5	3.0	13 ± 1
	Spot 7	2390	86.2	2.2	15 ± 2
	Spot 8	2660	85.7	2.6	11 ± 1
	Spot 9	2920	85.9	2.3	11 ± 1
	Spot 10	3190	86.3	1.9	12 ± 2
Sample 6	Spot 1	1330	88.9	0.8	85 ± 32
	Spot 2	1590	88.6	0.9	58 ± 18
	Spot 3	1860	88.6	0.4	65 ± 26
	Spot 4	2120	88.0	0.0	49 ± 17
	Spot 5	2390	88.0	0.7	32 ± 9
	Spot 6	2660	88.2	0.1	43 ± 17
	Spot 7	2920	88.5	0.1	45 ± 20
Sample 7	Spot 1	1330	86.7	2.7	26 ± 3
	Spot 2	1590	85.8	3.4	17 ± 2
Weighted Average (n = 36)					**14.3 ± 0.4**

[a]Retardation (Γ) between ordinary and extraordinary waves traversing the cell. All retardation values are assumed to have a measurement uncertainty of $\sigma_\Gamma = 50$ nm. [b]The angle (δ) formed between the alignment layers' easy axes. [c]The angle (γ) formed between the polarizer and analyzer that minimizes transmittance through the twisted nematic region when the easy axis of the bottom alignment layer lies parallel to the polarizer axis. Uncertainties in the measured angles (δ and γ) are $\sigma_\delta = \sigma_\gamma = 0.5°$.

Table S3. Azimuthal anchoring energy (W_{az}) of 4-cyano-4′-pentylbiphenyl (5CB) liquid crystals in cells prepared with *o*-1-carboranethiol (O1) SAMs.

O1		Γ (nm)[a]	δ (°)[b]	γ (°)[c]	W_{az} (μJ·m^{-2})
Sample 1	Spot 1	1060	84.7	3.5	22 ± 2
	Spot 2	1330	83.1	4.3	14 ± 1
	Spot 3	1590	84.8	2.9	16 ± 2
	Spot 4	1860	85.3	2.5	16 ± 2
	Spot 5	2120	85.4	2.2	14 ± 2
Sample 2	Spot 1	800	87.0	2.1	51 ± 8
	Spot 2	1060	86.7	3.4	29 ± 3
	Spot 3	1330	86.9	3.2	25 ± 3
	Spot 4	1590	86.9	2.5	24 ± 3
	Spot 5	1860	87.5	1.6	27 ± 5
	Spot 6	2120	87.2	0.1	35 ± 9
Sample 3	Spot 1	1330	88.3	3.5	30 ± 4
	Spot 2	1590	88.1	1.1	45 ± 11
	Spot 3	1860	88.7	2.4	30 ± 6
	Spot 4	2120	88.6	2.7	24 ± 4
	Spot 5	2390	89.4	2.3	30 ± 7
	Spot 6	2660	89.0	2.0	27 ± 6
Sample 4	Spot 1	2920	88.2	1.7	20 ± 4
	Spot 2	3190	88.0	1.4	19 ± 4
	Spot 3	3450	87.4	1.1	17 ± 3
Sample 5	Spot 1	530	81.9	0.5	46 ± 6
	Spot 2	800	85.3	4.8	27 ± 2
	Spot 3	1330	85.4	4.3	17 ± 2
	Spot 4	1590	85.4	2.3	19 ± 2
	Spot 5	1860	86.3	2.5	18 ± 2
	Spot 6	2120	85.7	3.7	12 ± 1
	Spot 7	2390	86.6	3.0	14 ± 2
	Spot 8	2660	86.8	2.6	13 ± 2
Sample 6	Spot 1	1060	85.7	3.7	24 ± 2
	Spot 2	1330	86.0	3.5	21 ± 2
	Spot 3	1590	86.0	2.8	19 ± 2
	Spot 4	1860	86.6	1.9	21 ± 3
	Spot 5	2120	86.4	2.9	15 ± 2
	Spot 6	2390	86.6	2.4	15 ± 2
	Spot 7	2660	86.6	2.4	14 ± 2
	Spot 8	2920	87.0	2.4	13 ± 2
	Spot 9	3190	87.2	1.9	14 ± 2
Weighted Average (n = 37)					**14.3 ± 0.4**

[a]Retardation (Γ) between ordinary and extraordinary waves traversing the cell. All retardation values are assumed to have a measurement uncertainty of $\sigma_\Gamma = 50$ nm. [b]The angle (δ) formed between the alignment layers' easy axes. [c]The angle (γ) formed between the polarizer and analyzer that minimizes transmittance through the twisted nematic region when the easy axis of the bottom alignment layer lies parallel to the polarizer axis. Uncertainties in the measured angles (δ and γ) are $\sigma_\delta = \sigma_\gamma = 0.5^\circ$.

Table S4. Azimuthal anchoring energy (W_{az}) of 4-cyano-4′-pentylbiphenyl (5CB) liquid crystals in cells prepared with *o*-9-carboranethiol (O9) SAMs.

O9		Γ (nm)[a]	δ (°)[b]	γ (°)[c]	W_{az} (μJ·m^{-2})
Sample 1	Spot 1	1060	87.4	2.4	40 ± 6
	Spot 2	1590	87.5	2.3	27 ± 4
	Spot 3	3190	88.6	0.7	32 ± 11
Sample 2	Spot 1	1060	90.3	2.0	110 ± 50
	Spot 2	1330	90.0	1.6	96 ± 41
	Spot 3	1590	89.9	2.4	54 ± 16
	Spot 4	1860	89.4	0.8	83 ± 43
Sample 3	Spot 1	800	85.4	5.5	26 ± 2
	Spot 2	1060	83.4	7.6	14 ± 1
	Spot 3	1330	84.8	5.6	14 ± 1
	Spot 4	1590	84.9	7.0	11 ± 1
	Spot 5	1860	85.3	5.1	11 ± 1
	Spot 6	2120	84.3	6.5	7.9 ± 0.5
Sample 4	Spot 1	1060	84.4	4.3	20 ± 2
	Spot 2	1330	84.6	3.8	17 ± 1
	Spot 3	1590	84.7	4.0	14 ± 1
	Spot 4	1860	85.2	3.0	14 ± 1
	Spot 5	2120	85.7	3.3	13 ± 1
	Spot 6	2390	85.2	3.4	11 ± 1
Sample 5	Spot 1	1060	81.5	9.9	11 ± 1
	Spot 2	1330	83.4	7.4	11 ± 1
	Spot 3	1590	83.1	7.7	8.9 ± 0.5
	Spot 4	1860	83.5	6.7	8.4 ± 0.5
	Spot 5	2120	83.2	7.4	6.8 ± 0.4
	Spot 6	2390	83.7	6.4	6.8 ± 0.4
	Spot 7	2660	83.3	7.0	5.6 ± 0.3
	Spot 8	2920	83.7	6.5	5.5 ± 0.3
	Spot 9	3190	83.7	6.1	5.2 ± 0.3
Weighted Average (*n* = 28)					**7.5 ± 0.1**

[a]Retardation (Γ) between ordinary and extraordinary waves traversing the cell. All retardation values are assumed to have a measurement uncertainty of $\sigma_\Gamma = 50$ nm. [b]The angle (δ) formed between the alignment layers' easy axes. [c]The angle (γ) formed between the polarizer and analyzer that minimizes transmittance through the twisted nematic region when the easy axis of the bottom alignment layer lies parallel to the polarizer axis. Uncertainties in the measured angles (δ and γ) are $\sigma_\delta = \sigma_\gamma = 0.5^\circ$.

Table S5. Azimuthal anchoring energy (W_{az}) of 4-cyano-4′-pentylbiphenyl (5CB) liquid crystals in cells prepared with *o*-9,12-carboranedithiol (9O12) SAMs.

9O12		Γ (nm)[a]	δ (°)[b]	γ (°)[c]	W_{az} (μJ·m^{-2})
Sample 1	Spot 1	800	86.2	4.6	31 ± 3
	Spot 2	1060	83.5	3.1	20 ± 2
	Spot 3	1330	84.7	0.3	28 ± 4
	Spot 4	1590	84.2	0.7	20 ± 2
	Spot 5	1860	85.5	2.0	17 ± 2
	Spot 6	2120	84.2	0.6	15 ± 2
	Spot 7	2390	85.9	0.8	18 ± 3
Sample 2	Spot 1	1590	89.9	3.4	38 ± 8
	Spot 2	1860	89.9	2.4	46 ± 13
	Spot 3	2120	88.7	2.2	29 ± 6
	Spot 4	2390	89.1	1.7	34 ± 9
	Spot 5	2660	89.9	2.4	32 ± 9
	Spot 6	2920	88.8	3.3	16 ± 3
Sample 3	Spot 1	1330	81.6	7.0	10 ± 1
	Spot 2	1590	80.9	7.5	7.8 ± 0.4
	Spot 3	1860	82.6	5.7	8.5 ± 0.5
	Spot 4	2120	81.9	6.5	6.6 ± 0.3
	Spot 5	2390	82.8	5.4	6.8 ± 0.4
	Spot 6	2660	81.8	5.8	5.6 ± 0.3
	Spot 7	2920	83.5	5.2	6.0 ± 0.4
	Spot 8	3190	81.5	6.4	4.3 ± 0.2
Sample 4	Spot 1	1330	85.8	5.8	16 ± 1
	Spot 2	1590	86.0	5.7	13 ± 1
	Spot 3	1860	85.8	3.8	14 ± 1
	Spot 4	2120	85.7	4.4	11 ± 1
	Spot 5	2390	86.0	2.9	13 ± 1
	Spot 6	2660	86.1	2.7	12 ± 1
	Spot 7	2920	85.9	2.4	11 ± 1
	Spot 8	3190	84.9	3.0	8.0 ± 0.7
Weighted Average (*n* = 29)					**6.7 ± 0.1**

[a]Retardation (Γ) between ordinary and extraordinary waves traversing the cell. All retardation values are assumed to have a measurement uncertainty of $\sigma_\Gamma = 50$ nm. [b]The angle (δ) formed between the alignment layers' easy axes. [c]The angle (γ) formed between the polarizer and analyzer that minimizes transmittance through the twisted nematic region when the easy axis of the bottom alignment layer lies parallel to the polarizer axis. Uncertainties in the measured angles (δ and γ) are $\sigma_\delta = \sigma_\gamma = 0.5^\circ$.

Oblique Gold Deposition.

Gold was deposited at an oblique angle (50° away from the normal) onto glass substrates, as shown in Figure S5. This angle describes the incidence angle of metal deposited in the center of the tilted substrate, located directly above the metal source. However, for extended substrates, this angle depends on the surface's distance away from the central deposition axis. Here, this deviation is no more than 6° from the intended deposition angle.

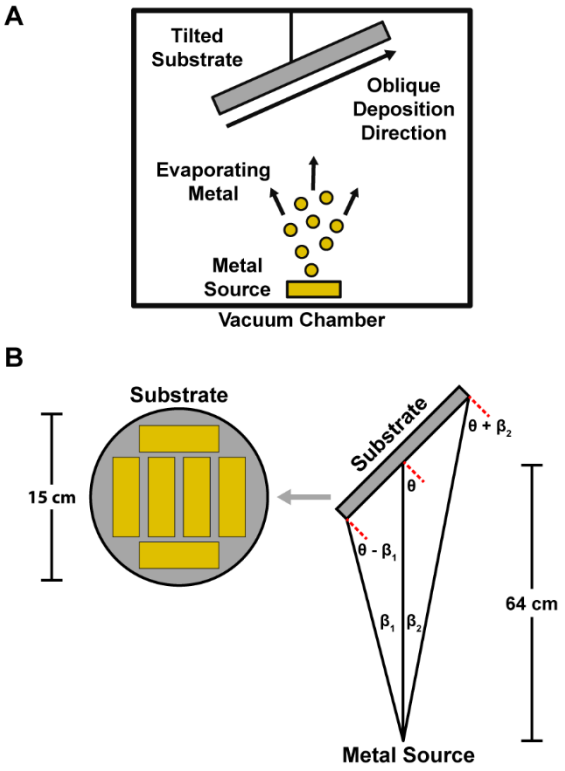

Figure S6. Schematic of oblique gold deposition. (A) Inside a vacuum chamber, gold is heated by an electron beam (not shown), causing it to evaporate from a source and deposit onto a tiled substrate located above. (B) Due to the non-zero widths and arrangement of glass, the deposition angle varies across the surface and between slides. Deviations from the intended angle ($\theta = 50°$) are expected to be, at most, $\beta_1 \approx \beta_2 \approx 6°$ for the dimensions and configuration used in this work.

Gaussian Calculations.

Molecular Dipole Moments. Table S6 summarizes the molecular dipole moments of **M9**, **M1**, **O9**, **O1**, **9O12**, and **1O2** calculated using density functional theory and the Gaussian 09 software package at the M062X level with the 6-311G** basis set. Dipole component vectors ($p_{||}$ and $p_{\perp}$) assume upright adsorption of the carboranethiol species on a gold surface.

Table S6. Molecular dipole moments (p) of carboranethiol and -dithiol isomers.

Isomer	Molecular Dipole Moment (D)		
	Magnitude	$p_{\|\|}$ [a]	$p_{\perp}$ [b]
M9[c]	3.94	1.38	3.70
M1[d]	2.20	2.13	-0.558
O9[e]	5.46	2.18	5.01
O1[f]	3.59	1.90	-3.05
9O12[g]	6.78	0.00	6.78
1O2[h]	3.20	0.00	-3.20

[a]In-plane dipole moment, parallel to the surface. [b]Out-of-plane dipole moment, normal to the surface. [c]*m*-9-carboranethiol (**M9**). [d]*m*-1-carboranethiol (**M1**). [e]*o*-9-carboranethiol (**O9**). [f]*o*-1-carboranethiol (**O1**). [g]*o*-9,12-carboranedithiol (**9O12**). [h]*o*-1,2-carboranedithiol (**1O2**).

Molecular Polarizability Tensor. The molecular polarizability tensors (**α**) of all six carboranethiols studied here were computed with the Gaussian 09 software package:

$$\boldsymbol{\alpha} = \begin{bmatrix} \boldsymbol{\alpha_{xx}} & \alpha_{xy} & \alpha_{xz} \\ \alpha_{xy} & \boldsymbol{\alpha_{yy}} & \alpha_{yz} \\ \alpha_{xz} & \alpha_{yz} & \boldsymbol{\alpha_{zz}} \end{bmatrix}$$

As described in the main text, Cartesian coordinate bases were chosen for each isomer based on its molecular symmetry and assumed upright adsorption onto underlying gold substrates. We found the polarizability tensors of each isomer to be *nearly* diagonalized in the chosen coordinate basis. As such, we consider only the carboranethiol polarizabilities along each of the coordinate axes (α_{xx}, α_{yy}, and α_{zz}), as summarized in Table S7.

Table S7. Molecular polarizabilities (α_{ii}) of carboranethiol and -dithiol isomers.

Isomer	Principal Polarizabilities (Å^3)		
	$\boldsymbol{\alpha_{xx}}$	$\boldsymbol{\alpha_{yy}}$	$\boldsymbol{\alpha_{zz}}$
M9[a]	19.4	19.2	24.3
M1[b]	19.4	19.6	23.6
O9[c]	19.5	19.8	24.0
O1[d]	19.4	19.7	23.7
9O12[e]	24.0	21.3	26.3
1O2[f]	23.4	21.3	26.4

[a]*m*-9-carboranethiol (**M9**). [b]*m*-1-carboranethiol (**M1**). [c]*o*-9-carboranethiol (**O9**). [d]*o*-1-carboranethiol (**O1**). [e]*o*-9,12-carboranedithiol (**9O12**). [f]*o*-1,2-carboranedithiol (**1O2**).

Optimized Molecular Geometries and Dipoles. Computed values of the molecular dipole vectors and polarizability tensors depend on the optimized orientation of the thiol moiety (S–H bond) in each carboranethiol isomer. However, the hydrogen on the molecule's thiol functionality is lost during chemisoption onto the gold surface (becoming -thiol*ate*). As such, the

dipoles and polarizabilities computed for these structures do not accurately reflect those of the actual *adsorbed* molecule. To account for this change in molecular structure upon chemisorption, we computed the molecular dipoles and polarizabilities of each isomer as the average of those values from multiple (nearly degenerate) conformations of each isomer. Each molecular conformation was distinguished by the initial value of the carborane–sulfur–hydrogen dihedral angle in the unoptimized structure, reflecting the rotational symmetry of the thiol moieties in each isomer (five-fold and two-fold symmetries in the cases of mono- and dithiol species, respectively). Averaging effectively eliminates the thiol contributions to the in-plane molecular dipole and polarizability. The tables below present the atomic coordinates of each structure after optimization, labeled with the initial thiol dihedral angles. During optimization, atoms in each structure were allowed to relax into their lowest energy positions with the exceptions of dihedral angles denoted by "F." In these "frozen" structures, the value of the thiol dihedral angle was not optimized in order to maintain the desired molecular symmetry. These molecular conformations do not represent energetically optimized structures. If optimized without restrictions, an unfavorable interaction between the electron deficient carbon atoms in the carborane cage and the polar S–H bond would cause the thiol dihedral angle to deviate significantly from its initial value and disrupt the symmetry of the model. As such, these structures were used with only partial structural optimization. We reiterate, however, that the adsorbed molecule does not possess the carborane–sulfur–hydrogen dihedral angle left unoptimized here. In the cases of carboranedithiol isomers, the two conformations are distinguished by an "M" (or its absence) in the table heading. These conformations are mirror-symmetric versions of the fully optimized structures, reflecting the bilateral symmetry of the dithiol species.

M9 (0°) Energy: -730.121306 E_h

Atom	Position Coordinates (Å)		
	X	Y	Z
B	0.112328	-0.4994	-1.422584
B	-1.393971	-1.240065	-0.862785
B	0.131359	1.192437	-0.906861
B	1.065263	-0.016128	-0.000362
B	0.115184	-1.520253	0.025303
B	-1.360695	1.500783	-0.024783
B	0.132472	1.22187	0.865364
B	0.113277	-0.451841	1.437922
B	-1.393854	-1.210304	0.904755
C	-1.319917	0.443261	1.287942
H	0.545346	-0.778257	-2.48149
H	0.633748	-2.580157	0.042517
H	0.562947	2.034117	-1.609023
H	-1.965234	2.508414	-0.040872
H	0.54684	-0.695522	2.505253
H	0.564102	2.086491	1.539219
H	-1.978863	-1.950561	1.609212
H	-1.979496	-2.003201	-1.541961
B	-2.308671	-0.005531	0.000636
C	-1.321212	0.400457	-1.301621
H	-1.816124	0.69738	-2.21541
H	-3.478525	0.103897	-0.00055
H	-1.813884	0.770472	2.191888
S	2.927707	-0.084822	-0.000618
H	3.119158	1.243927	0.010164

M9 (72°, F) Energy: -730.121033 E_h

Atom	Position Coordinates (Å)		
	X	Y	Z
B	-0.107117	1.489342	-0.232513
B	1.407478	1.341038	0.681516
B	-0.124049	0.23107	-1.485054
B	-1.064653	0.023934	0.015641
B	-0.099851	0.71243	1.358978
B	1.361379	-0.70142	-1.331054
B	-0.144687	-1.331282	-0.667711
B	-0.12732	-1.032239	1.085953
B	1.396634	-0.222552	1.496113
C	1.298797	-1.351164	0.224497
H	-0.52408	2.559672	-0.494616
H	-0.619224	1.205486	2.295336
H	-0.556541	0.456686	-2.556171
H	1.961981	-1.17588	-2.222646
H	-0.567869	-1.855249	1.805434
H	-0.587619	-2.333491	-1.100653
H	1.982563	-0.502995	2.478173
H	2.004867	2.297188	1.021268
B	2.308309	-0.015211	0.004933
C	1.326391	0.944199	-0.974342
H	1.825069	1.607339	-1.666786
H	3.477842	-0.077383	-0.089676
H	1.778651	-2.3084	0.37096
S	-2.928377	0.083104	-0.008285
H	-3.103354	-1.236404	0.156996

M9 (144°) Energy: -730.121494 E_h

Atom	Position Coordinates (Å)		
	X	Y	Z
B	0.115038	-0.247782	1.486599
B	-1.389949	0.678357	1.355552
B	0.123054	-1.48438	0.211914
B	1.064465	0.002157	0.005351
B	0.124923	1.340214	0.714753
B	-1.376141	-1.318956	-0.701775
B	0.11839	-0.660627	-1.352864
B	0.124748	1.079833	-1.040262
B	-1.378709	1.50418	-0.204677
C	-1.321241	0.238252	-1.340791
H	0.547625	-0.521716	2.54693
H	0.654528	2.273163	1.206619
H	0.543676	-2.564026	0.422844
H	-1.989435	-2.205945	-1.168597
H	0.560845	1.805697	-1.859864
H	0.546522	-1.092243	-2.360608
H	-1.95537	2.496756	-0.466906
H	-1.972793	1.023154	2.318847
B	-2.308361	0.019761	0.005842
C	-1.322341	-0.970733	0.950342
H	-1.818246	-1.668702	1.609747
H	-3.479332	-0.064677	-0.041078
H	-1.815604	0.39646	-2.288699
S	2.927231	-0.080245	0.011026
H	3.116097	1.237102	-0.155119

M9 (216°) Energy: -730.121477 E_h

Atom	Position Coordinates (Å)		
	X	Y	Z
B	-0.124597	1.086609	-1.033387
B	1.379	1.505224	-0.195074
B	-0.118495	-0.651983	-1.35705
B	-1.06448	0.002546	0.005272
B	-0.124588	1.335919	0.723338
B	1.37587	-1.314633	-0.71017
B	-0.123365	-1.485513	0.202565
B	-0.115139	-0.256927	1.48488
B	1.390147	0.669584	1.359842
C	1.322024	-0.976836	0.944141
H	-0.560253	1.817911	-1.848367
H	-0.653903	2.265837	1.221148
H	-0.546574	-1.077265	-2.367499
H	1.988938	-2.198763	-1.182581
H	-0.548029	-0.537573	2.543311
H	-0.544392	-2.566275	0.40671
H	1.973231	1.007945	2.325235
H	1.955856	2.499308	-0.451081
B	2.308375	0.019311	0.005949
C	1.321141	0.246531	-1.339235
H	1.815492	0.410709	-2.286122
H	3.479296	-0.064984	-0.041786
H	1.817685	-1.679032	1.599219
S	-2.927112	-0.080227	0.011179
H	-3.116187	1.236947	-0.157323

M9 (288°, F) Energy: -730.121018 E_h

Atom	Position Coordinates (Å)		
	X	Y	Z
B	0.127109	-1.028763	1.089338
B	-1.396597	-0.217475	1.496728
B	0.144485	-1.33351	-0.663294
B	1.064659	0.023668	0.015675
B	0.099985	0.716784	1.356662
B	-1.361459	-0.705701	-1.328731
B	0.124055	0.226207	-1.485686
B	0.10728	1.488266	-0.237305
B	-1.407242	1.34333	0.677033
C	-1.326282	0.941081	-0.977404
H	0.567346	-1.849514	1.81159
H	0.619366	1.212841	2.291423
H	0.587356	-2.337148	-1.092998
H	-1.961899	-1.18308	-2.21888
H	0.524468	2.557678	-0.502845
H	0.556726	0.44801	-2.557526
H	-2.004556	2.300618	1.013718
H	-1.982526	-0.494497	2.479764
B	-2.308381	-0.014963	0.00492
C	-1.298953	-1.350281	0.228872
H	-1.778958	-2.306977	0.378352
H	-3.477942	-0.077368	-0.089287
H	-1.824922	1.602042	-1.671963
S	2.928368	0.083084	-0.008571
H	3.103583	-1.235965	0.160289

M1 (0°) Energy: -730.087128 E_h

Atom	Position Coordinates (Å)		
	X	Y	Z
B	-0.006375	-2.29319	0
B	-0.459726	-1.363726	1.437534
B	-0.459726	-1.363726	-1.437534
B	1.223728	-1.384639	-0.891013
B	1.223728	-1.384639	0.891013
B	-1.182181	0.149111	-0.892629
B	0.48693	0.123759	-1.444556
B	1.518888	0.119307	0
B	0.48693	0.123759	1.444556
B	0.024159	0.931496	0
S	0.083814	2.73539	0
H	-0.167801	-3.459906	0
H	2.067258	-1.914586	1.522554
H	2.067258	-1.914586	-1.522554
H	-0.921438	-1.89197	-2.383428
H	-2.065369	0.721566	-1.41736
H	-1.248119	2.907203	0
H	2.505108	0.764927	0
H	0.772391	0.773359	-2.38313
H	0.772391	0.773359	2.38313
H	-0.921438	-1.89197	2.383428
B	-1.182181	0.149111	0.892629
C	-1.363978	-1.267222	0
H	-2.347043	-1.716478	0
H	-2.065369	0.721566	1.41736

M1 (72°) Energy: -730.086719 E_h

Atom	Position Coordinates (Å)		
	X	Y	Z
B	-2.292922	0.008104	0.001202
B	-1.351529	1.477475	-0.319174
B	-1.366046	-1.382705	-0.59101
B	-1.384156	-0.997583	1.139364
B	-1.379755	0.774135	1.307899
B	0.135976	-0.774191	-1.272138
B	0.130363	-1.474634	0.347126
B	0.113794	-0.145286	1.521828
B	0.140591	1.378588	0.620809
C	0.931724	-0.00727	0.019786
S	2.734587	-0.082457	0.004335
H	-3.460917	0.028378	-0.149555
H	-1.904398	1.332514	2.204708
H	-1.913163	-1.710976	1.915695
H	-1.899745	-2.282461	-1.131451
H	0.704107	-1.213897	-2.20145
H	2.914123	1.246972	-0.047249
H	0.765394	-0.243144	2.497542
H	0.774677	-2.442482	0.538475
H	0.790995	2.289757	0.99037
H	-1.872732	2.469755	-0.681038
B	0.147192	0.989834	-1.103327
C	-1.281687	0.132558	-1.354182
H	-1.738415	0.228793	-2.329122
H	0.71892	1.595678	-1.932806

M1 (144°) Energy: -730.087017 E_h

Atom	Position Coordinates (Å)		
	X	Y	Z
B	-2.293109	0.017216	0.001486
B	-1.360217	0.669061	-1.354707
B	-1.373176	-1.313809	0.72623
B	-1.380499	0.282112	1.492663
B	-1.361946	1.51154	0.203894
B	0.134621	-1.474987	-0.174985
B	0.12058	-0.64859	1.381965
B	0.132345	1.09069	1.051876
B	0.143705	1.333847	-0.710188
C	0.932064	0.001243	0.013466
S	2.734744	-0.080646	-0.013276
H	-3.462148	-0.082814	-0.103683
H	-1.873994	2.567262	0.326204
H	-1.906431	0.46288	2.532934
H	-1.911767	-2.294378	1.094128
H	0.69376	-2.483458	-0.404766
H	2.912093	1.23049	0.212904
H	0.787364	1.799228	1.729461
H	0.766035	-1.098792	2.256971
H	0.799147	2.184055	-1.196109
H	-1.887121	0.999917	-2.354646
B	0.135456	-0.251719	-1.468886
C	-1.285171	-0.976151	-0.939641
H	-1.745808	-1.684442	-1.613714
H	0.7028	-0.536976	-2.456955

M1 (288°) Energy: -730.086719 E_h

Atom	Position Coordinates (Å)		
	X	Y	Z
B	2.292922	0.008104	0.001202
B	1.366046	-1.382705	-0.59101
B	1.351529	1.477475	-0.319174
B	1.379755	0.774135	1.307899
B	1.384156	-0.997583	1.139364
B	-0.147192	0.989834	-1.103327
B	-0.140591	1.378588	0.620809
B	-0.113794	-0.145286	1.521828
B	-0.130363	-1.474634	0.347126
C	-0.931724	-0.00727	0.019786
S	-2.734587	-0.082457	0.004335
H	3.460917	0.028378	-0.149555
H	1.913163	-1.710976	1.915695
H	1.904398	1.332514	2.204708
H	1.872732	2.469755	-0.681038
H	-0.71892	1.595678	-1.932806
H	-2.914123	1.246972	-0.047249
H	-0.765394	-0.243144	2.497542
H	-0.790995	2.289757	0.99037
H	-0.774677	-2.442482	0.538475
H	1.899745	-2.282461	-1.131451
B	-0.135976	-0.774191	-1.272138
C	1.281687	0.132558	-1.354182
H	1.738415	0.228793	-2.329123
H	-0.704107	-1.213897	-2.20145

M1 (216°) Energy: -730.087017 E_h

Atom	Position Coordinates (Å)		
	X	Y	Z
B	2.293109	0.017216	0.001486
B	1.373176	-1.313809	0.72623
B	1.360217	0.669061	-1.354707
B	1.361946	1.51154	0.203894
B	1.380499	0.282112	1.492663
B	-0.135456	-0.251719	-1.468886
B	-0.143705	1.333847	-0.710188
B	-0.132345	1.09069	1.051876
B	-0.12058	-0.64859	1.381965
C	-0.932064	0.001243	0.013466
S	-2.734744	-0.080646	-0.013276
H	3.462148	-0.082814	-0.103683
H	1.906431	0.46288	2.532934
H	1.873994	2.567262	0.326204
H	1.887121	0.999917	-2.354646
H	-0.7028	-0.536976	-2.456955
H	-2.912093	1.23049	0.212904
H	-0.787364	1.799228	1.729461
H	-0.799147	2.184055	-1.196109
H	-0.766035	-1.098792	2.256971
H	1.911767	-2.294378	1.094128
B	-0.134621	-1.474987	-0.174985
C	1.285171	-0.976151	-0.939641
H	1.745808	-1.684442	-1.613714
H	-0.69376	-2.483458	-0.404766

O9 (0°) Energy: -730.094599 E_h

Atom	Position Coordinates (Å)		
	X	Y	Z
B	0.542841	0.916284	0
B	1.083677	-0.516861	0.891108
B	1.083677	-0.516861	-0.891108
B	-0.350068	0.357946	-1.448694
B	-1.227917	0.912141	0
B	-0.350068	0.357946	1.448694
B	-0.350068	-1.400445	-1.44712
B	-1.778961	-0.51853	-0.88931
B	-1.778961	-0.51853	0.88931
B	-0.350068	-1.400445	1.44712
C	0.464261	-1.805781	0
C	-1.152496	-1.811643	0
H	-0.338989	0.957717	2.463669
H	-1.861642	1.90792	0
H	-0.338989	0.957717	-2.463669
H	2.096703	-0.672771	-1.472741
H	-0.344929	-2.189553	-2.319443
H	-2.788995	-0.685343	1.471825
H	-2.788995	-0.685343	-1.471825
H	-0.344929	-2.189553	2.319443
H	2.096703	-0.672771	1.472741
H	0.945015	-2.77296	0
H	-1.627003	-2.78164	0
S	1.505326	2.513933	0
H	2.719823	1.944986	0

O9 (72°) Energy: -730.0948 E_h

Atom	Position Coordinates (Å)		
	X	Y	Z
B	1.064565	-0.007598	0.027938
B	0.134338	-0.810727	-1.258873
B	0.143316	0.956589	-1.144262
B	0.12899	1.404468	0.576582
B	0.107352	-0.099379	1.526885
B	0.118428	-1.470079	0.38939
B	-1.357907	1.47662	-0.363681
B	-1.387357	0.81101	1.280286
B	-1.393438	-0.959102	1.166661
B	-1.371079	-1.41017	-0.549248
C	-1.287983	0.089642	-1.355432
C	-2.1468	0.007	0.006049
H	0.620355	-2.509586	0.634328
H	0.616099	-0.1701	2.588755
H	0.640394	2.4016	0.948246
H	0.552876	1.598589	-2.043203
H	-2.01611	2.381335	-0.726398
H	-2.075255	-1.594078	1.887139
H	-2.064889	1.354372	2.07603
H	-2.038895	-2.255197	-1.021612
H	0.540415	-1.333767	-2.232292
H	-1.853578	0.151736	-2.27357
H	-3.220411	0.019033	-0.108353
S	2.928301	-0.082815	0.011069
H	3.11884	1.243098	-0.068264

O9 (144°) Energy: -730.094923 E_h

Atom	Position Coordinates (Å)		
	X	Y	Z
B	1.065074	0.002122	0.023183
B	0.131243	-1.41369	-0.487481
B	0.136771	0.050894	-1.495056
B	0.133297	1.456604	-0.419792
B	0.121093	0.852553	1.261458
B	0.109025	-0.925264	1.219941
B	-1.363324	0.942262	-1.193502
B	-1.374003	1.431907	0.509057
B	-1.393051	-0.034717	1.511838
B	-1.37787	-1.444914	0.443129
C	-1.288402	-0.758845	-1.122134
C	-2.145982	0.016273	0.004706
H	0.614246	-1.594332	2.048968
H	0.631342	1.453155	2.140577
H	0.649726	2.46875	-0.739337
H	0.546208	-0.002402	-2.597481
H	-2.024455	1.432524	-2.033672
H	-2.075201	-0.078673	2.471003
H	-2.04357	2.353589	0.807858
H	-2.050969	-2.399175	0.583474
H	0.529885	-2.428919	-0.932385
H	-1.855808	-1.278364	-1.880146
H	-3.220111	-0.040784	-0.090707
S	2.927638	-0.075125	-0.021175
H	3.121548	1.183284	0.401344

O9 (216°) Energy: -730.094923 E_h

Atom	Position Coordinates (Å)		
	X	Y	Z
B	-1.065074	0.002122	0.023183
B	-0.136771	0.050906	-1.495056
B	-0.131243	-1.413686	-0.487492
B	-0.109025	-0.925274	1.219934
B	-0.121093	0.852544	1.261465
B	-0.133297	1.456607	-0.41978
B	1.37787	-1.444918	0.443117
B	1.393051	-0.034729	1.511837
B	1.374003	1.431903	0.509069
B	1.363324	0.942272	-1.193494
C	1.288402	-0.758837	-1.12214
C	2.145982	0.016273	0.004706
H	-0.649726	2.468756	-0.739317
H	-0.631342	1.453138	2.140589
H	-0.614246	-1.594348	2.048955
H	-0.529884	-2.428912	-0.932404
H	2.050969	-2.39918	0.583455
H	2.04357	2.353583	0.807876
H	2.075201	-0.078692	2.471003
H	2.024455	1.43254	-2.033661
H	-0.546207	-0.002381	-2.597482
H	1.855808	-1.278349	-1.880156
H	3.220111	-0.040784	-0.090707
S	-2.927638	-0.075125	-0.021175
H	-3.121547	1.183287	0.401335

O9 (288°) Energy: -730.094802 E_h

Atom	Position Coordinates (Å)		
	X	Y	Z
B	-1.064536	-0.007643	0.027622
B	-0.143157	0.954654	-1.145996
B	-0.134092	-0.812797	-1.257729
B	-0.11843	-1.469495	0.391623
B	-0.107604	-0.096901	1.526948
B	-0.129094	1.405411	0.574124
B	1.3712	-1.410938	-0.546798
B	1.393238	-0.957141	1.168435
B	1.387126	0.813125	1.279144
B	1.357892	1.475956	-0.36596
C	1.288246	0.087446	-1.355482
C	2.146739	0.007061	0.006297
H	-0.640899	2.402939	0.944164
H	-0.616934	-0.165838	2.588657
H	-0.620565	-2.508485	0.63831
H	-0.539891	-1.337663	-2.230285
H	2.039156	-2.25677	-1.017509
H	2.064568	1.358071	2.07388
H	2.075001	-1.591204	1.889772
H	2.016151	2.380114	-0.729966
H	-0.552612	1.595351	-2.045913
H	1.85402	0.148077	-2.273603
H	3.220378	0.018915	-0.107836
S	-2.928263	-0.082801	0.01103
H	-3.118797	1.243109	-0.068106

O1 (36°, F) Energy: -730.060377 E_h

Atom	Position Coordinates (Å)		
	X	Y	Z
B	-2.30685	0.033849	-0.027383
B	-1.328504	1.451868	-0.443923
B	-1.348304	0.036824	-1.512923
B	-1.395652	-1.419808	-0.50585
B	-1.421482	-0.895385	1.195554
B	-1.385301	0.882307	1.234811
B	0.121861	-0.902669	-1.218768
B	0.092666	-1.464022	0.464238
B	0.088928	-0.049452	1.542483
B	0.14777	1.401038	0.53479
C	0.094886	0.79469	-1.064737
C	0.919258	-0.049581	0.053283
S	2.718972	-0.073822	0.019126
H	-3.485049	0.078135	-0.074749
H	-1.884132	1.531127	2.084568
H	-1.955341	-1.531757	2.03398
H	-1.904568	-2.414726	-0.884153
H	-1.701203	0.148253	-2.631379
H	0.80432	-1.367142	-2.054957
H	2.852449	1.198599	-0.389503
H	0.749676	-0.06051	2.516726
H	0.743071	-2.408403	0.737016
H	0.836606	2.332059	0.745296
H	-1.669078	2.503683	-0.850972
H	0.699184	1.32844	-1.784302

O1 (108°) Energy: -730.064318 E_h

Atom	Position Coordinates (Å)		
	X	Y	Z
B	-2.306267	0.00202	-0.040636
B	-1.339281	0.75951	-1.314289
B	-1.341434	-1.003303	-1.132273
B	-1.38994	-1.384791	0.599931
B	-1.423673	0.156642	1.487431
B	-1.3781	1.484951	0.304025
B	0.139879	-1.475167	-0.273575
B	0.084712	-0.75728	1.347705
B	0.097254	1.006965	1.163099
B	0.143612	1.386444	-0.572655
C	0.086061	-0.135484	-1.328059
C	0.921732	0.001967	0.076731
S	2.710186	-0.082665	-0.015151
H	-3.48456	0.000161	-0.102136
H	-1.873222	2.53962	0.490543
H	-1.958579	0.268377	2.533586
H	-1.896601	-2.376141	0.990377
H	-1.693514	-1.691212	-2.021323
H	0.821799	-2.385723	-0.575103
H	2.902823	1.240347	0.102007
H	0.752809	1.668739	1.885281
H	0.738169	-1.2607	2.187737
H	0.829823	2.215287	-1.049843
H	-1.687246	1.253901	-2.325501
H	0.704755	-0.228859	-2.20906

O1 (180°) Energy: -730.060695 E_h

Atom	Position Coordinates (Å)		
	X	Y	Z
B	-0.027166	-2.3076	0
B	-1.220813	-1.348573	0.888096
B	-1.220813	-1.348573	-0.888096
B	0.460222	-1.389453	-1.442525
B	1.500646	-1.406745	0
B	0.460222	-1.389453	1.442525
B	-0.427438	0.12721	-1.45233
B	1.249234	0.101204	-0.890081
B	1.249234	0.101204	0.890081
B	-0.427438	0.12721	1.45233
C	-1.329101	0.090015	0
C	0.059761	0.918474	0
S	-0.089639	2.717101	0
H	-0.081066	-3.486251	0
H	0.759699	-1.890494	2.467891
H	2.560175	-1.927466	0
H	0.759699	-1.890494	-2.467891
H	-2.178727	-1.703393	-1.474799
H	-0.821022	0.810995	-2.323021
H	1.238015	2.913728	0
H	2.03239	0.761416	1.473893
H	2.03239	0.761416	-1.473893
H	-0.821022	0.810995	2.323021
H	-2.178727	-1.703393	1.474799
H	-2.230976	0.686226	0

O1 (324°, F) Energy: -730.060377 E_h

Atom	Position Coordinates (Å)		
	X	Y	Z
B	2.30685	0.033849	-0.027383
B	1.348304	0.036824	-1.512923
B	1.328504	1.451868	-0.443923
B	1.385301	0.882307	1.234811
B	1.421482	-0.895385	1.195553
B	1.395652	-1.419808	-0.505851
B	-0.14777	1.401038	0.53479
B	-0.088928	-0.049452	1.542483
B	-0.092666	-1.464022	0.464238
B	-0.121862	-0.902669	-1.218768
C	-0.094886	0.79469	-1.064737
C	-0.919258	-0.049581	0.053283
S	-2.718972	-0.073822	0.019126
H	3.485049	0.078135	-0.074749
H	1.904568	-2.414726	-0.884153
H	1.955341	-1.531757	2.03398
H	1.884132	1.531127	2.084568
H	1.669078	2.503683	-0.850972
H	-0.836606	2.332059	0.745296
H	-2.852449	1.198599	-0.389503
H	-0.743071	-2.408403	0.737016
H	-0.749675	-0.060511	2.516726
H	-0.80432	-1.367142	-2.054957
H	1.701203	0.148253	-2.631379
H	-0.699184	1.32844	-1.784302

O1 (252°) Energy: -730.064318 E_h

Atom	Position Coordinates (Å)		
	X	Y	Z
B	2.306267	0.00202	-0.040636
B	1.341434	-1.003303	-1.132273
B	1.339281	0.75951	-1.314289
B	1.3781	1.484951	0.304025
B	1.423673	0.156642	1.487431
B	1.38994	-1.384791	0.599931
B	-0.143612	1.386444	-0.572655
B	-0.097254	1.006965	1.163099
B	-0.084712	-0.75728	1.347705
B	-0.139879	-1.475167	-0.273575
C	-0.086061	-0.135484	-1.328059
C	-0.921732	0.001967	0.076731
S	-2.710186	-0.082665	-0.015151
H	3.48456	0.000161	-0.102136
H	1.896601	-2.376141	0.990377
H	1.958579	0.268377	2.533586
H	1.873222	2.53962	0.490543
H	1.687246	1.253901	-2.325501
H	-0.829823	2.215287	-1.049843
H	-2.902823	1.240347	0.102007
H	-0.738169	-1.2607	2.187737
H	-0.752809	1.668739	1.885281
H	-0.821799	-2.385723	-0.575103
H	1.693514	-1.691212	-2.021323
H	-0.704755	-0.228859	-2.20906

9O12 (±45°) Energy: -1128.303216 E_h

Atom	Position Coordinates (Å)		
	X	Y	Z
B	0.535882	0.897152	0.003172
B	-0.902604	1.433649	-0.889713
B	-0.902743	1.435681	0.882307
B	-0.015434	0.000035	1.441041
B	0.535975	-0.897034	0.003185
B	-0.014025	0.000031	-1.437214
B	-1.77226	-0.000068	1.446071
B	-0.902593	-1.435704	0.882248
B	-0.90249	-1.433668	-0.889672
B	-1.779833	-0.000048	-1.445936
C	-2.193546	0.806423	-0.003676
C	-2.193468	-0.806438	-0.003681
H	0.590193	0.000054	-2.450789
H	0.586889	0.000075	2.456094
H	-1.059389	2.445061	1.469722
H	-2.555257	-0.000124	2.323534
H	-1.054603	-2.441755	-1.477865
H	-1.059401	-2.444977	1.469814
H	-2.558908	-0.000119	-2.326608
H	-1.054576	2.441888	-1.477674
H	-3.16217	1.284042	0.000373
H	-3.161933	-1.284378	0.000376
S	2.111133	-1.884974	-0.066359
S	2.111078	1.885012	-0.066373
H	1.928085	-2.521092	1.101578
H	1.928399	2.520681	1.101867

1O2 (±45°) Energy: -1128.239475 E_h

Atom	Position Coordinates (Å)		
	X	Y	Z
B	2.335055	0.883042	0.006139
B	0.913764	1.438384	-0.885606
B	0.904109	1.440401	0.884974
B	1.765084	-0.000011	1.443479
B	2.335052	-0.883037	0.006125
B	1.77926	0.000017	-1.434374
B	0.000667	0.000003	1.415744
B	0.904088	-1.440395	0.884941
B	0.91377	-1.438375	-0.885644
B	0.006779	0.00001	-1.418041
C	-0.409429	0.860743	-0.002616
C	-0.409434	-0.860747	-0.00264
H	2.354583	0.000047	-2.464216
H	2.330562	-0.000056	2.479187
H	0.734061	2.43911	1.487298
H	-0.78023	-0.000066	2.298465
H	0.746364	-2.436059	-1.487646
H	0.7341	-2.439103	1.487277
H	-0.771712	0.000081	-2.302012
H	0.746422	2.436074	-1.487613
H	3.322752	1.528521	0.012549
H	3.322727	-1.528551	0.012538
S	-1.969506	1.717671	-0.080274
S	-1.969479	-1.717719	-0.080256
H	-2.045457	-1.962396	1.23783
H	-2.045378	1.962987	1.237691

9O12 (±45°, M) Energy: -1128.303216 E_h

Atom	Position Coordinates (Å)		
	X	Y	Z
B	-0.535882	0.897152	0.003172
B	0.902743	1.435681	0.882307
B	0.902604	1.433649	-0.889713
B	0.014025	0.000031	-1.437214
B	-0.535975	-0.897034	0.003185
B	0.015434	0.000035	1.441041
B	1.779833	-0.000048	-1.445936
B	0.90249	-1.433668	-0.889672
B	0.902593	-1.435704	0.882248
B	1.77226	-0.000068	1.446071
C	2.193546	0.806423	-0.003676
C	2.193468	-0.806438	-0.003682
H	-0.586889	0.000075	2.456094
H	-0.590193	0.000054	-2.450789
H	1.054576	2.441888	-1.477674
H	2.558908	-0.000119	-2.326608
H	1.059401	-2.444977	1.469814
H	1.054603	-2.441755	-1.477865
H	2.555257	-0.000124	2.323534
H	1.059389	2.445061	1.469722
H	3.16217	1.284042	0.000373
H	3.161933	-1.284378	0.000376
S	-2.111133	-1.884974	-0.066359
S	-2.111078	1.885012	-0.066373
H	-1.928085	-2.521092	1.101578
H	-1.928399	2.520681	1.101867

1O2 (±45°, M) Energy: -1128.239475 E_h

Atom	Position Coordinates (Å)		
	X	Y	Z
B	-2.335055	0.883042	0.006139
B	-0.904109	1.440401	0.884974
B	-0.913764	1.438384	-0.885606
B	-1.77926	0.000017	-1.434374
B	-2.335052	-0.883037	0.006125
B	-1.765084	-0.000011	1.443479
B	-0.006779	0.00001	-1.418041
B	-0.91377	-1.438375	-0.885644
B	-0.904088	-1.440395	0.884941
B	-0.000667	0.000003	1.415744
C	0.409429	0.860743	-0.002616
C	0.409434	-0.860747	-0.00264
H	-2.330562	-0.000056	2.479187
H	-2.354583	0.000047	-2.464216
H	-0.746422	2.436074	-1.487613
H	0.771712	0.000081	-2.302012
H	-0.7341	-2.439103	1.487277
H	-0.746364	-2.436059	-1.487646
H	0.78023	-0.000066	2.298465
H	-0.734061	2.43911	1.487298
H	-3.322752	1.528521	0.012549
H	-3.322727	-1.528551	0.012538
S	1.969506	1.717672	-0.080274
S	1.969479	-1.717719	-0.080256
H	2.045457	-1.962396	1.23783
H	2.045377	1.962988	1.237691

References.

(S1) Toyooka, T.; Chen, G.; Takezoe, H.; Fukuda, A. *Jpn. J. Appl. Phys.* **1987**, *26* (Part 1, No. 12), 1959–1966.
(S2) Belyaev, B. A.; Drokin, N. A.; Shabanov, V. F.; Shepov, V. N. *Phys. Solid State* **2000**, *42*, 577–579.
(S3) Li, J.; Wen, C.-H.; Gauza, S.; Lu, R.; Wu, S.-T. *J. Disp. Technol.* **2005**, *1*, 51–61.
(S4) Clare, B. H.; Guzmán, O.; de Pablo, J. J.; Abbott, N. L. *Langmuir* **2006**, *22*, 4654–4659.
(S5) Maurel, P.; Price, A. H. *J. Chem. Soc., Faraday Trans. 2* **1973**, *69*, 1486–1490.
(S6) de Jeu, W. H. *Physical Properties of Liquid Crystalline Materials*; Gordon and Breach: New York, 1980.
(S7) Nakata, M.; Zanchetta, G.; Buscaglia, M.; Bellini, T.; Clark, N. A. *Langmuir* **2008**, *24*, 10390–10394.
(S8) Sørensen, B. E. *Eur. J. Mineral.* **2013**, *25*, 5–10.